Supplementary Materials and Methods

siRNA transfections

Transfections were performed using Lipofectamine® RNAiMAX (Invitrogen) according to the manufacturer's instructions. siGENOME SMARTpool siRNA (Dharmacon) were used for depletion.

Table SI 1 Sequences of siRNAs used in this study.

Non-targeting #5 (NT5)	UGGUUUACAUGUCGACUAA
p63	D-003330-05: CAUCAUGUCUGGACUAUUU D-003330-06: CAAACAAGAUUGAGAUUAG D-003330-07: GCACACAGACAAAUGAAUU D-003330-08: CGACAGUCUUGUACAAUUU
BHLHE40	D-010318-01: GAAAGGAUCGGCGCAAUUA D-010318-02: CGAAACAGGUCAAGAGAUG D-010318-03: GAACAUCUCAAACUUACAA D-010318-04: GCACUAACAAACCUAAUUG
HIF1A	D-004018-01: GGACACAGAUUUAGACUUG D-004018-03: GAUGGAAGCACUAGACAAA D-004018-05: CGUGUUAUCUGUCGCUUUG D-004018-27: GAUGAAAGAAUUACCGAAU
RXRA	D-003443-06: GGGAGAAGGUCUAUGCGUC D-003443-07: CAGGUGAACUCCUCCCUCA D-003443-08: CGAACGACCCUGUCACCAA D-003443-09: UUGCCAAGCAGCCGACAAA

Proliferation and sphere formation assays

100,000 (L3.6pl) or 50,000 (BxPC-3, Panc-1, MIA Paca-2) cells were reverse transfected in duplicates in 12- or 24-well plates, respectively, with NT5 or p63 siRNAs. After 48 h, cells were fixed with methanol for 10 min and stained with 1% crystal violet in 20% ethanol for 20 min and then washed and scanned. Relative area fraction was measured using ImageJ and plotted using GraphPad Prism version 5.04 (GraphPad Software, Inc.). Same protocol was followed for proliferation assay after knockdown of p63, BHLHE40, HIF1A, and RXRA. For sphere formation assay, cells were transfected on day 1 as previously mentioned and in duplicates for NT5 and p63 and then 500 cells were seeded in ultra-low attachment surface 96-well plate (n=12 for each duplicate, n=24 for each condition). Plates were scanned after 7 days by Celigo® S imaging cytometer (Nexcelom Bioscience LLC).

Protein extraction and western blot analysis

Protein was extracted by washing cells with PBS and suspending in RIPA buffer (1X PBS, 0.5% sodium deoxycholate 0.1% SDS, 1% NP-40) supplemented with 100 µM β-glycerophosphate disodium salt hydrate (BGP), 100 µM N-ethylmaleimide, and protease inhibitors (100 µM Pefabloc, 1 µM aprotonin, 1 µM leupeptin). Protein lysates were solubilized by sonication using a Bioruptor Pico (Diagenode) for 10 cycles (30 s on/off). Laemli buffer (375 mM Tris/HCl, 10% SDS, 30% glycerol, 0.02% bromophenol blue, 9.3% DTT) was added to lysates before separation with a 7% polyacrylamide gel for evaluation of expression of the levels of p63 in multiple pancreatic cell line and transcription factors in L3.6pl and 12% for p63 knockdown validation. Protein was then transferred onto nitrocellulose membranes that were incubated with primary antibodies in 5% milk in TBS-T overnight and then with secondary antibodies for one hour. Protein bands were visualized using Bio-

Rad ChemiDocTM imager. Antibodies used were: HSC70 Santa-Cruz (#sc-7298) in 1:10,000 dilution in 5% Milk in TBS-T, p63 (4A4) Santa-Cruz (#sc-8431) in 1:1000 which detects all isoforms of p63 (1-4), BHLHE40 Novus (NB100-1800) in 1:1000, HIF1A (D2U3T) Cell signaling #14179 in 1:1000, RXRA (D-20) Santa-Cruz (#sc-553) in 1:1000. Secondary antibodies used were anti-rabbit IgG and anti-mouse IgG from Dianova (211-032-171 and 115-035-174, respectively).

RNA isolation and quantitative real-time PCR (qPCR)

RNA isolation and quantitative real-time PCR was performed as previously described (5, 6). Briefly, triplicates for each condition were harvested 48 h after transfection by QIAzol® reagent (Qiagen). Reverse transcription of 1 µg RNA was performed using M-MuLV reverse transcriptase (NEB) and random primers and the resultant complementary DNA was quantified by quantitative real-time PCR (qPCR) using a CFX Connect™ Real-Time System (Bio-Rad). Gene expression levels were normalized relative to an internal unregulated reference gene, GAPDH. Protocol for qPCR runs included 2 min denaturation at 95ºC, 40 cycles of 10 s at 95ºC followed by 30 s at 60 ºC. Primers (Supplementary Table SI 2) were designed using the NCBI primerblast design tool (https://www.ncbi.nlm.nih.gov/tools/primer-blast/) and were ordered from Sigma-Aldrich (Germany).

Table SI 2 Sequences of primers used to check gene expression in this study.

Name	Forward Primer	Reverse Primer	Source
GAPDH	ATGGGGAAGGTGAAGGTCG	GGGGTCATTGATGGCAACAATA	Tian et al. 2013(7)
DeltaNp63	AGAGAGAGGGACTTGAGTTCTG	GCTCACTAAATTGAGTCTGGGC	Scheel et al. 2009(8)
TAp63	GTTATTACCGATCCACCATGTCC	CCCAGATATGCTGGAAAACCT	Beyer et al. 2011(9)
FAT2	CCCACAGTGTTCACAGCTTCT	TCCAAGTCTGTGGCAGAAACC	This Study
NECTIN1	GCGAGTTTGCTACCTTCCCT	ATTGGTGGGTTTGGCCATCA	This Study
HIF1A	TGCTTACACACAGAAATGGCCT	TACGTGAATGTGGCCTGTGC	This Study
BHLHE40	ATTAACGAGTGCATCGCCCA	TTCCAAGTGACCCAAAGTTGTAAGT	This Study
RXRA	GCCGGGAAGGTTCGCTAAG	GTGTCCCCGATGAGCTTGAA	This Study

Chromatin Immunoprecipitation (ChIP)

Briefly, cells were crosslinked with 1% formaldehyde for 20 minutes and quenched by glycine (125mM final concentration). Cells were scraped and nuclear pellets were prepared in and washed with the nuclear preparation buffer (150 mM NaCl, 20 mM EDTA, 50 mM Tris-HCl (pH 7.5), 0.5% v/v NP-40, 1% v/v Triton-X-100, 20 mM NaF). Samples were then sonicated in sonication buffer (150mM NaCl, 20 mM EDTA, 50 mM Tris-HCl (pH 8), 1% v/v NP-40, 0.5% v/v sodium deoxycholate, 20 mM NaF, 0.1% SDS) for 30 cycles (in L3.6pl) or 25 cycles (in BxPC-3 and Panc-1) using a Bioruptor Pico (Diagenode) and a cycle setting of 30 s on/off. Consequently, samples were precleared by incubation with 50% slurry of Sepharose 4B (GE Healthcare), centrifuged and supernatants were incubated with antibody overnight. Antibodies included p63 (1µg; clone 4A4, sc-8431, Santa-Cruz), H3K27ac (1µg; 196-050, Diagenode), BRD4 (2µg; C15410337, Diagenode), BHLHE40 (2µg; NB100-1800, Novus), HIF1A (10µl; #14179, Cell Signaling), RXRA (1µg; sc-553, Santa-Cruz), and control rabbit IgG (1µg; C15410206, Diagenode). Protein A- (for rabbit antibodies) or Protein G- (for mouse antibodies, 4A4 p63) Sepharose beads were added to samples and incubated for 2 h, then washed, de-crosslinked, and DNA was extracted. For ChIP-sequencing, samples were performed in duplicate for each

condition. For ChIP-qPCR for validation of enrichment and loss upon depletion of p63, cells were seeded in triplicate and transfected with siRNA and nuclear pellets harvested after 48 h. Quantitative PCR conditions were the same as gene expression studies but the cycle number was increased to 46. Primers were designed for regions of positive enrichment for p63 and H3K27ac and the first intron of *OLIG2* was used as a negative site for enrichment to ensure specificity of signal (oligonucleotide sequences for ChIP validation Table SI 3). The signal was normalized to input DNA and presented as percent input for duplicates or triplicates in each condition.

Table SI 3 Primers sequences for checking enrichment in ChIP-qPCR experiments in this study.

Name	Forward Primer	Reverse Primer	Source
p63_FAT2 -3.7kb	GCCTCCATGTAACTCCCAGC	CCTGTGTGTTGTTAGCCACCT	This Study
ac_FAT2 -3.7kb	TTCTTTCCTCCTGACTGTGCTTC	GTTGAACAGGTAGCAAGTGGTAGA	This Study
p63_FAT2 -46.5kb	CAGACCCTGCGTTCTGTCTT	TGATTCATGACCAGGGGTGC	This Study
ac_FAT2 -46.5kb	AGCTGGAAACCGACAGCTTG	GCAGTTCCATTGTCGCTGTG	This Study
p63_NECTIN1 31.8 kb	AGGCTGGAAGGCATCTTGC	CATTGTGCAGGTGACATCGC	This Study
ac_NECTIN1 31.8 kb	GTGCTTCCTGCTTCCCAGAAT	CCTGGTAGATAGAAGGTATTCAGCC	This Study
p63_NECTIN1 36.2 kb	TGGGGTCTTTCCCATGCTTC	CCCAGTGACTCCTGAAACCC	This Study
ac_NECTIN1 36.2 kb	TCCCTGGGGGAGAAAGTACAA	CACATGTGTTAACTGTTCTTGCCA	This Study
p63_HIF1A -62.2 kb	TACTGTGGCGGTGAAATCAACT	AGTATCTACCCTGCTCCTTGGT	This Study
ac_HIF1A -62.2 kb	CGGCATTTCAGCTTTGGCAG	CCCAGTGCCACAGAACAAAGA	This Study
OLIG2 H3K27me3	GTCACCAACGCTCCCTGAAAT	CTGCACGCGGGTACCTATAAT	This Study

Assay for transposase-accessible chromatin (ATAC)

Briefly, 50,000 L3.6pl cells were trypsinized and washed twice with cold PBS. Then cells were re-suspended in lysis buffer (10mM Tris-HCl pH 7.5, 10mM NaCl, 3mM $MgCl_2$, 0.1% IGEPAL CA-630), incubated for 15 min on a rotating wheel at 4 C, followed by centrifugation and then resuspended in 50 µl of transposition mix composed of 2.5 µl of TDE1 (Nextera Tn5 Transposase), 25 µl TD (2x reaction buffer) in nuclease free water (Nextera DNA Library Prep Kit, FC-121-1030, Illumina). DNA extraction was immediately preformed after 30 min of incubating the transposition reaction at 37 C. MinElute PCR Purification kit (Qiagen) was used for DNA extraction and following the instructions of the manufacturer. Experiment was done in duplicates.

Library preparation for RNA, ChIP, and ATAC-seq and next-generation sequencing

Libraries for DNA from ChIP were made using the Microplex Library Preparation kit v2 (Diagenode) according to the manufacturer's instructions. ATAC libraries were made using the Nextera DNA Library Prep Kit and the libraries were amplified for 15 cycles in total of: 98 C for 10 sec, 63 C for 30 sec, and 72 C for 60 sec. The quality of the libraries was verified using the high sensitivity DNA kit (Agilent) on the Agilent Bioanalyzer 2100. RNA- and ChIP-seq samples were sequenced (single-end 50 bp) on a HiSeq4000 (Illumina) in the Transcriptome and Genome Analysis Laboratory (TAL) at the University Medical Center Göttingen. ATAC-seq samples were sequenced (single-end 50bp) on HiSeq2000 (Illumina). Images of sequences were converted into bcl files (BaseCaller software, Illumina) and demultiplexed to fastq files by CASAVA v1.8.2.

Bioinformatic analysis for ChIP and ATAC-sequencing

Hierarchical clustering was performed for H3K27ac regions by seqMINER/1.3.4 using KMeans enrichment linear as clustering normalization (10, 11). Differential binding analysis was performed to identify differentially occupied regions in L3.6pl and BxPC-3 compared to Panc-1 using the Bioconductor R package Diffbind run on R version 3.3.1 according to the instruction manual (12). Genomic Regions Enrichment of Annotations Tool (GREAT) analysis was used to identify associated genes with regions identified by differential binding analysis and hierarchical clustering. multiBigwigSummary BED-file and plotPCA tools in DEEPTOOLS/2.4.0 were used to plot the principle component analysis for the H3K27ac profiles on differentially occupied regions for the 24 patient-derived xenografts. Heatmaps and average profiles for occupancy were generated using the computeMatrix and plotHeatmap tools on the European UseGalaxy server and the reference point mode were selected as the peak center (13). Super enhancers were identified using the ROSE algorithm by using the H3K27ac regions as input files and BRD4 compared to input as intensity files, ignoring regions that are 2500 bp around TSS and keeping stitching of regions to the default 12.5 kb (14, 15). Cluster of regulatory elements (COREs) were identified using the CREAM R package according to instruction manual (16). To identify common super enhancers, we used the multiinter tool in BEDTOOLS/2.24 and the VennDiagram R package to generate the Venn diagrams (17, 18). Upstream activators for super enhancer regions were identified using EnrichR web-based interface (19). Occupancy regions of HIF1A, BHLHE40, RXRA were extracted from the ReMAP database v1.2 (20, 21).

Bioinformatic analysis for RNA-seq

Hierarchical clustering by Euclidean distance for FPKM and Z-score was performed using cluster 3.0 (22) and the resulting heatmaps viewed using TreeView 3.0 (23). Z-scores were calculated by subtracting the mean of FPKM values in all cells and dividing by the deviation. FPKM values for expressed genes in any condition were used as input for gene set enrichment analysis (GSEA) which was performed using default settings (1000 permutations and for a maximum size of sets of 1000) (24). Unexpressed genes with very low FPKM values in both conditions (siControl and sip63) were disregarded to avoid bias. For heatscatter plot for signal of p63 at TSS, the TSS with the highest signal was taken. The transcription factor and target gene network was visualized using Cytoscape v3.6.1 and extended by the TF-target query of the iRegulon app (25, 26). FPKM values for genes associated with H3K27ac gained regions were plotted as log2 (FPKM+1) values in L3.6pl, BxPC-3, and Panc-1 using the boxplot command in R.

Accession numbers

Accession numbers for datasets used in this study are listed in Table SI 4 for ChIP-seq datasets and Table SI 5 for RNA-seq datasets.

Table SI 4 Accession numbers for next-generation datasets used in this study (ChIP and ATAC-seq)

Name	Data Type	Database	Accession Number	Replicates	Source
BxPC-3_H3K27ac	ChIP-seq	ArrayExpress	E-MTAB-7034	2	This Study
L3.6pl_H3K27ac	ChIP-seq	ArrayExpress	E-MTAB-7034	2	This Study
Panc-1_H3K27ac	ChIP-seq	ArrayExpress	E-MTAB-7034	2	This Study
AO.IP_H3K27ac	ChIP-seq	ArrayExpress	E-MTAB-5632	1	Lomberk et al 2018(27)
1.033_H3K27ac	ChIP-seq	ArrayExpress	E-MTAB-5632	1	Lomberk et al 2018
1.03_H3K27ac	ChIP-seq	ArrayExpress	E-MTAB-5632	1	Lomberk et al 2018
1.048_H3K27ac	ChIP-seq	ArrayExpress	E-MTAB-5632	1	Lomberk et al 2018
foei8_H3K27ac	ChIP-seq	ArrayExpress	E-MTAB-5632	1	Lomberk et al 2018
2.087_H3K27ac	ChIP-seq	ArrayExpress	E-MTAB-5632	1	Lomberk et al 2018
2.029_H3K27ac	ChIP-seq	ArrayExpress	E-MTAB-5632	1	Lomberk et al 2018
1.037_H3K27ac	ChIP-seq	ArrayExpress	E-MTAB-5632	1	Lomberk et al 2018
AM.IP_H3K27ac	ChIP-seq	ArrayExpress	E-MTAB-5632	1	Lomberk et al 2018
D.IP_H3K27ac	ChIP-seq	ArrayExpress	E-MTAB-5632	1	Lomberk et al 2018
B.Tim_H3K27ac	ChIP-seq	ArrayExpress	E-MTAB-5632	1	Lomberk et al 2018
AH.IP_H3K27ac	ChIP-seq	ArrayExpress	E-MTAB-5632	1	Lomberk et al 2018
3.076_H3K27ac	ChIP-seq	ArrayExpress	E-MTAB-5632	1	Lomberk et al 2018
2.116_H3K27ac	ChIP-seq	ArrayExpress	E-MTAB-5632	1	Lomberk et al 2018
2.099_H3K27ac	ChIP-seq	ArrayExpress	E-MTAB-5632	1	Lomberk et al 2018
2.083_H3K27ac	ChIP-seq	ArrayExpress	E-MTAB-5632	1	Lomberk et al 2018
2.058_H3K27ac	ChIP-seq	ArrayExpress	E-MTAB-5632	1	Lomberk et al 2018
2.045_H3K27ac	ChIP-seq	ArrayExpress	E-MTAB-5632	1	Lomberk et al 2018
1.119_H3K27ac	ChIP-seq	ArrayExpress	E-MTAB-5632	1	Lomberk et al 2018
1.064_H3K27ac	ChIP-seq	ArrayExpress	E-MTAB-5632	1	Lomberk et al 2018
1.053_H3K27ac	ChIP-seq	ArrayExpress	E-MTAB-5632	1	Lomberk et al 2018
1.052_H3K27ac	ChIP-seq	ArrayExpress	E-MTAB-5632	1	Lomberk et al 2018
1.043_H3K27ac	ChIP-seq	ArrayExpress	E-MTAB-5632	1	Lomberk et al 2018
1.042_H3K27ac	ChIP-seq	ArrayExpress	E-MTAB-5632	1	Lomberk et al 2018
L3.6pl_p63	ChIP-seq	ArrayExpress	E-MTAB-7034	1	This study
BxPC-3_p63	ChIP-seq	ArrayExpress	E-MTAB-7034	1	This study
L3.6pl_BRD4	ChIP-seq	ArrayExpress	E-MTAB-7034	2	This study
BxPC-3_BRD4	ChIP-seq	ArrayExpress	E-MTAB-7034	2	This study
Panc-1_BRD4	ChIP-seq	ArrayExpress	E-MTAB-7034	2	This study
L3.6pl_ATAC	ATAC-seq	ArrayExpress	E-MTAB-7035	2	This study
BxPC-3_input	ChIP-seq	ArrayExpress	E-MTAB-7034	1	This study
L3.6pl_input	ChIP-seq	ArrayExpress	E-MTAB-7034	2	This study
Panc-1_input	ChIP-seq	ArrayExpress	E-MTAB-7034	1	This study
AO.IP_input	ChIP-seq	ArrayExpress	E-MTAB-7034	1	Lomberk et al 2018
1.033_input	ChIP-seq	ArrayExpress	E-MTAB-5632	1	Lomberk et al 2018
foei8_input	ChIP-seq	ArrayExpress	E-MTAB-5632	1	Lomberk et al 2018
1.064_input	ChIP-seq	ArrayExpress	E-MTAB-5632	1	Lomberk et al 2018
2.045_input	ChIP-seq	ArrayExpress	E-MTAB-5632	1	Lomberk et al 2018
2.116_input	ChIP-seq	ArrayExpress	E-MTAB-5632	1	Lomberk et al 2018
MIA PACA-2_ H3K27ac	ChIP-seq	GEO	GSM1574239	1	Diaferia et al 2016 (28)

Table SI 5 Accession numbers for next-generation datasets used in this study (RNA-seq)

Name	Data Type	Database	Accession Number	Replicates	Source
BxPC-3_siControl	mRNA-seq	ArrayExpress	E-MTAB-7033	3	This Study
BxPC-3_sip63	mRNA-seq	ArrayExpress	E-MTAB-7033	3	This Study
L3.6_siControl	mRNA-seq	ArrayExpress	E-MTAB-7033	3	This Study
L3.6pl_sip63	mRNA-seq	ArrayExpress	E-MTAB-7033	3	This study
Panc1_sicontrol	mRNA-seq	GEO	GSE90566	3	Mishra et al. 2017
AO.IP	mRNA-seq	ArrayExpress	E-MTAB-5639	1	Lomberk et al 2018
1.033	mRNA-seq	ArrayExpress	E-MTAB-5639	1	Lomberk et al 2018
1.03	mRNA-seq	ArrayExpress	E-MTAB-5639	1	Lomberk et al 2018
1.048	mRNA-seq	ArrayExpress	E-MTAB-5639	1	Lomberk et al 2018
foei8	mRNA-seq	ArrayExpress	E-MTAB-5639	1	Lomberk et al 2018
2.087	mRNA-seq	ArrayExpress	E-MTAB-5639	1	Lomberk et al 2018
2.029	mRNA-seq	ArrayExpress	E-MTAB-5639	1	Lomberk et al 2018
1.037	mRNA-seq	ArrayExpress	E-MTAB-5639	1	Lomberk et al 2018
AM.IP	mRNA-seq	ArrayExpress	E-MTAB-5639	1	Lomberk et al 2018
D.IP	mRNA-seq	ArrayExpress	E-MTAB-5639	1	Lomberk et al 2018
B.Tim	mRNA-seq	ArrayExpress	E-MTAB-5639	1	Lomberk et al 2018
AH.IP	mRNA-seq	ArrayExpress	E-MTAB-5639	1	Lomberk et al 2018
3.076	mRNA-seq	ArrayExpress	E-MTAB-5639	1	Lomberk et al 2018
2.116	mRNA-seq	ArrayExpress	E-MTAB-5639	1	Lomberk et al 2018
2.099	mRNA-seq	ArrayExpress	E-MTAB-5639	1	Lomberk et al 2018
2.083	mRNA-seq	ArrayExpress	E-MTAB-5639	1	Lomberk et al 2018
2.058	mRNA-seq	ArrayExpress	E-MTAB-5639	1	Lomberk et al 2018
2.045	mRNA-seq	ArrayExpress	E-MTAB-5639	1	Lomberk et al 2018
1.119	mRNA-seq	ArrayExpress	E-MTAB-5639	1	Lomberk et al 2018
1.064	mRNA-seq	ArrayExpress	E-MTAB-5639	1	Lomberk et al 2018
1.053	mRNA-seq	ArrayExpress	E-MTAB-5639	1	Lomberk et al 2018
1.052	mRNA-seq	ArrayExpress	E-MTAB-5639	1	Lomberk et al 2018
1.043	mRNA-seq	ArrayExpress	E-MTAB-5639	1	Lomberk et al 2018
1.042	mRNA-seq	ArrayExpress	E-MTAB-5639	1	Lomberk et al 2018

Supplementary Figure Legends

Supplementary Figure 1. (**A**) Heatmap showing the enrichment of H3K27ac at the concatenated and merged peaks for BxPC-3, L3.6pl, and Panc-1. Peaks were clustered into 3 groups based on K-Means hierarchical clustering normalized to linear enrichment. Cluster 3 shows more enrichment in L3.6pl and BxPC-3 compared to Panc-1. (**B**) Box plot showing log2 (FPKM+1) values for associated genes with gained H3K27ac in Panc-1, BxPC-3, and L3.6pl. n=3. * P-value <= 0.05, ** P-value <=0.01, *** P-value <=0.001. (**C**) Associated genes with the H3K27ac gained regions also showing validated targets of deltaNp63 as the top hit. (**D**) Occupancy profiles of H3K27ac at TSS of TAp63 and deltaNp63 for 6 xenografts, L3.6pl, BxPC3, Panc-1, and MIA Paca-2. (**E**) Bar plot showing the FPKM values of p63 (all isoforms) calculated by CUFFLINKS/2.2.1 in the 24 PDX samples. (**F**) Heatmap depicting the general expression patterns of p63 in all pancreatic cancer cell lines listed in the Morpheus database. (**G**) Heatmap showing the Z-scores of the FPKM values for the squamous gene signature in the 6 PDX samples shown in A. Hierarchical clusters for samples based on the expression underscores the increased expression of the signature apparent in the 3 three squamous PDX-samples. (**H**) GSEA plots comparing the enrichment of genes associated with favorable outcome in pancreatic cancer in BxPC-3 compared to Panc-1 using the FPKM values of all expressed genes with the NES (normalized enrichment score) and FDR (false-discovery rate) indicated on the graph.

Supplementary Figure 2. (**A**) Gene expression analysis of deltaNp63 upon depletion of p63 in Panc-1 after 48 h showing no detected expression. (**B**) Crystal violet staining showing the proliferation of cells after 48 h of depletion of p63 compared to control for Panc-1 cells with relative area fraction shown in the bar graph. Data are represented as mean ± SEM. n = 2. * P-value <= 0.05, ** P-value <=0.01, *** P-value <=0.001, **** P-value <=0.0001. (**C**) Gene expression analysis of TAp63 in MIA Paca-2 upon depletion of p63 after 48 h shown as relative mRNA expression and normalized to the unregulated housekeeping gene (GAPDH). n = 3. * P-value <= 0.05, ** P-value <=0.01, *** P-value <=0.001, **** P-value <=0.0001. (**D**) Crystal violet staining showing the proliferation of cells after 48 h of depletion of p63 compared to control for MIA Paca-2 cells with relative area fraction shown in the bar graph. Data are represented as mean ± SEM. n = 2. * P-value <= 0.05, ** P-value <=0.01, *** P-value <=0.001, **** P-value <=0.0001. (**E**) Representative pictures of spheres formed by L3.6pl, BxPC-3, and MIA Paca-2 cells. (**F-G**) GSEA report for enriched genes upon downregulation of p63 in L3.6pl with pathways enriched in the control (F) and sip63 (G).

Supplementary Figure 3. (**A**) Average binding profiles and heatmaps depicting the p63, H3K27ac occupancy, and open chromatin defined by ATAC-seq at the p63 regions in L3.6pl. (**B**) Venn diagram showing the overlap between down regulated genes and genes associated with p63 regions occupied with H3K27ac and regions that are not marked by H3KK27ac. Associated genes were identified using the beta-minus method using the galaxy cistrome. A slight bias for p63 dependence is shown for genes that associated with p63 peaks marked with H3K27ac. (**C**) Heat scatter plot showing the relationship between occupancy of p63 at TSS and the gene regulation upon knockdown of p63 showing a lack of correlation between TSS occupancy and dependence. (**D**) Venn Diagram showing the overlap between p63 regions and TSS in L3.6pl. (**E-F**) Enhancers in BxPC-3 and Panc-1 ranked

based on BRD4 signal intensity using the ROSE algorithm defining 624 super enhancers. BxPC-3 shows common high ranking super enhancers with L3.6pl while Panc-1 has distinct highly ranking super enhancers. (**G**) Venn diagram showing the overlap between super enhancers defined by ROSE, clusters of regulatory elements by CREAM, and p63 peaks. (**H**) Bar graph showing the percentages of and COREs that are occupied by any number of peaks of deltaNp63 (>=1), by at least more than 2 peaks, or 3 peaks, with grey depicting regions that are common between SEs and COREs.

Supplementary Figure 4. (**A**) Box plot showing the log2 fold change upon depletion of p63 for genes associated with SEs and COREs (defined based on H3K27ac or ATAC peaks) and their subgroups based on the number of p63 peaks they contain. (**B**) Scatter plot for FPKM values in control and sip63 samples for genes associated with super enhancers (red), COREs (blue), and both (yellow). (**C**) ChEA and ENCODE consensus output for super enhancer regions in L3.6pl defined by erichr. (**D**) Directed acyclic graph for gene ontology pathways associated with genes related to super enhancers in L3.6pl with squamous cell carcinoma as a high significant hit (**E-F**) Venn diagrams depicting the overlap between H3K27ac gained regions, super enhancers in L3.6 and the three squamous xenografts in J and the common regions between them with the SEs of other xenografts lacking deltaNp63.

Supplementary Figure 5. (**A**) Occupancy profiles at *HIF1A* for p63 in L3.6pl and BxPC-3, ATAC seq in L3.6pl, H3K27ac in L3.6pl and BxPC-3, and 6 xenografts. (**B**) Gene expression analysis for *HIF1A* by qRT-PCR of deltaNp63 upon depletion of p63 after 48 hours shown as relative mRNA expression and normalized to the unregulated housekeeping gene (*GAPDH*). n = 3. * P-value <= 0.05, ** P-value <=0.01, *** P-value <=0.001. (**C-D**) ChIP-qPCR analysis validating enrichment of p63 (C) and H3K27ac (D) at the highlighted region in A (-62.2 kb from TSS of *HIF1A*) in the control and p63 depletion after 48 hours. n=3 (one sample for p63 in p63 was disregarded because of decreased DNA amount to ensure significance in the decrease of the enrichment is not due to an outlier). Data are represented as mean ± SEM. n = 2. * P-value <= 0.05, ** P-value <=0.01, *** P-value <=0.001. (**E**) ChIP-qPCR analysis validating lack of enrichment of p63 and H3K27ac at a negative region (OLIG2 H3K27me3) to ensure specific signal. (**F**) Occupancy profiles at *NECTIN1* for p63 in L3.6pl and BxPC-3, ATAC seq in L3.6pl, H3K27ac in L3.6pl and BxPC-3, and 6 xenografts. (**G**) Gene expression analysis for *NECTIN1* following depletion of p63 for 48 h shown as relative mRNA expression and normalized to an unregulated housekeeping gene (*GAPDH*). n = 3. * P-value <= 0.05, ** P-value <=0.01, *** P-value <=0.001, **** P-value <=0.0001. (**H**) Validation of p63 and H3K27ac enrichment by ChIP-qPCR at the two highlighted regions in F (+31.8 kb and +36.2 kb from TSS of *NECTIN1*) in control and p63-depleted cells after 48 h. n=2-3. Data are represented as mean ± SEM. n = 2. * P-value <= 0.05, ** P-value <=0.01, *** P-value <=0.001, **** P-value <=0.0001.

Supplementary Figure 6. (**A-H**) Kaplan-Meier plots showing the percent survival in pancreatic cancer patients (TCGA database) expressing high and low levels of the gene named on the top of each graph with p-value indicated on graph (Mantel-Cox test).

Supplementary Figure 7. (**A**) Kaplan-Meier plot showing the percent survival in pancreatic cancer patients (TCGA database) expressing high and low levels of BHLHE40 and FAT2 with p-value indicated on graph. (**B**) Heatmap depicting the gene expression patterns of transcription

factorsassociated with the squamous subtype-specific super enhancers, namely HIF1A, BHLHE40, and RXRA in different pancreatic cancer cell lines (Morpheus database). (**C**) Western blot analysis for p63, BHLHEH440, HIF1A, and RXRA in L3.6pl 48 h after depletion of p63, BHLHE40, HIF1A, RXRA. HSC70 is shown as loading control. (**D-E**) Crystal violet staining showing the proliferation of cells after 48 h of depletion of p63, BHLEH40, HIF1A, and RXRA compared to control with relative area fraction shown in the bar graph. Data are represented as mean ± SEM. n = 2. * P-value <= 0.05, ** P-value <=0.01, *** P-value <=0.001, **** P-value <=0.0001. (**F**) Representative pictures of cell morphology after 48 h knockdown of p63 and BHLHE40 compared to control L3.6pl cells (10X). Scale bar on bottom right corner.

SI Dataset (Dataset S1-S7) provided in Excel and txt. format

Dataset S1: H3K27ac gained regions in L3.6pl and BxPC-3

Dataset S2: Genes associated with H3K27ac gained regions in L3.6pl and BxPC-3

Dataset S3: Squamous gene signature (Bailey et al.)

Dataset S4: GSEA table for enrichment of C2 pathways in siControl compared to sip63 in L3.6pl

Dataset S5: GSEA table for enrichment of C2 pathways in sip63 compared to siControl in L3.6pl

Dataset S6: Squamous subtype-specific super enhancers

Dataset S7: Top regulated genes upon depletion of p63 in L3.6pl and BxPC-3

Supplementary References

1. Tan M, Bian J, Guan K, & Sun Y (2001) p53CP is p51/p63, the third member of the p53 gene family: partial purification and characterization. *Carcinogenesis* 22(2):295-300.
2. Nekulova M*, et al.* (2013) Characterization of specific p63 and p63-N-terminal isoform antibodies and their application for immunohistochemistry. *Virchows Arch* 463(3):415-425.
3. Bortoluzzi MC, Yurgel LS, Dekker NP, Jordan RC, & Regezi JA (2004) Assessment of p63 expression in oral squamous cell carcinomas and dysplasias. *Oral Surg Oral Med Oral Pathol Oral Radiol Endod* 98(6):698-704.
4. Pruneri G*, et al.* (2005) The transactivating isoforms of p63 are overexpressed in high-grade follicular lymphomas independent of the occurrence of p63 gene amplification. *J Pathol* 206(3):337-345.
5. Mishra VK*, et al.* (2017) Histone deacetylase class-I inhibition promotes epithelial gene expression in pancreatic cancer cells in a BRD4- and MYC-dependent manner. *Nucleic Acids Res* 45(11):6334-6349.
6. Prenzel T*, et al.* (2011) Estrogen-dependent gene transcription in human breast cancer cells relies upon proteasome-dependent monoubiquitination of histone H2B. *Cancer Res* 71(17):5739-5753.
7. Tian B*, et al.* (2013) CDK9-dependent transcriptional elongation in the innate interferon-stimulated gene response to respiratory syncytial virus infection in airway epithelial cells. *J Virol* 87(12):7075-7092.
8. Scheel AH, Beyer U, Agami R, & Dobbelstein M (2009) Immunofluorescence-based screening identifies germ cell associated microRNA 302 as an antagonist to p63 expression. *Cell Cycle* 8(9):1426-1432.
9. Beyer U, Moll-Rocek J, Moll UM, & Dobbelstein M (2011) Endogenous retrovirus drives hitherto unknown proapoptotic p63 isoforms in the male germ line of humans and great apes. *Proc Natl Acad Sci U S A* 108(9):3624-3629.
10. Ye T*, et al.* (2011) seqMINER: an integrated ChIP-seq data interpretation platform. *Nucleic Acids Res* 39(6):21.
11. Ye T, Ravens S, Krebs AR, & Tora L (2014) Interpreting and visualizing ChIP-seq data with the seqMINER software. *Methods Mol Biol*:0512-0516_0518.
12. Ross-Innes CS*, et al.* (2012) Differential oestrogen receptor binding is associated with clinical outcome in breast cancer. *Nature* 481(7381):389-393.
13. Afgan E*, et al.* (2016) The Galaxy platform for accessible, reproducible and collaborative biomedical analyses: 2016 update. *Nucleic Acids Res* 44(W1):W3-W10.
14. Loven J*, et al.* (2013) Selective inhibition of tumor oncogenes by disruption of super-enhancers. *Cell* 153(2):320-334.
15. Whyte WA*, et al.* (2013) Master transcription factors and mediator establish super-enhancers at key cell identity genes. *Cell* 153(2):307-319.
16. Madani Tonekaboni SA, Mazrooei P, Kofia V, Haibe-Kains B, & Lupien M (2017) CREAM: Clustering of genomic REgions Analysis Method. *bioRxiv*.
17. Quinlan AR & Hall IM (2010) BEDTools: a flexible suite of utilities for comparing genomic features. *Bioinformatics* 26(6):841-842.
18. Chen H & Boutros PC (2011) VennDiagram: a package for the generation of highly-customizable Venn and Euler diagrams in R. *BMC Bioinformatics* 12(35):1471-2105.
19. Kuleshov MV*, et al.* (2016) Enrichr: a comprehensive gene set enrichment analysis web server 2016 update. *Nucleic Acids Res* 44(W1):3.
20. Griffon A*, et al.* (2015) Integrative analysis of public ChIP-seq experiments reveals a complex multi-cell regulatory landscape. *Nucleic Acids Res* 43(4):3.
21. Cheneby J, Gheorghe M, Artufel M, Mathelier A, & Ballester B (2018) ReMap 2018: an updated atlas of regulatory regions from an integrative analysis of DNA-binding ChIP-seq experiments. *Nucleic Acids Res* 46(D1):D267-D275.
22. de Hoon MJ, Imoto S, Nolan J, & Miyano S (2004) Open source clustering software. *Bioinformatics* 20(9):1453-1454.
23. Saldanha AJ (2004) Java Treeview--extensible visualization of microarray data. *Bioinformatics* 20(17):3246-3248.
24. Subramanian A*, et al.* (2005) Gene set enrichment analysis: a knowledge-based approach for interpreting genome-wide expression profiles. *Proc Natl Acad Sci U S A* 102(43):15545-15550.
25. Shannon P*, et al.* (2003) Cytoscape: a software environment for integrated models of biomolecular interaction networks. *Genome Res* 13(11):2498-2504.
26. Janky R*, et al.* (2014) iRegulon: from a gene list to a gene regulatory network using large motif and track collections. *PLoS Comput Biol* 10(7).
27. Lomberk G*, et al.* (2018) Distinct epigenetic landscapes underlie the pathobiology of pancreatic cancer subtypes. *Nature Communications* 9(1):1978.
28. Diaferia GR*, et al.* (2016) Dissection of transcriptional and cis-regulatory control of differentiation in human pancreatic cancer. *Embo J* 35(6):595-617.

Supplementary Figure 1

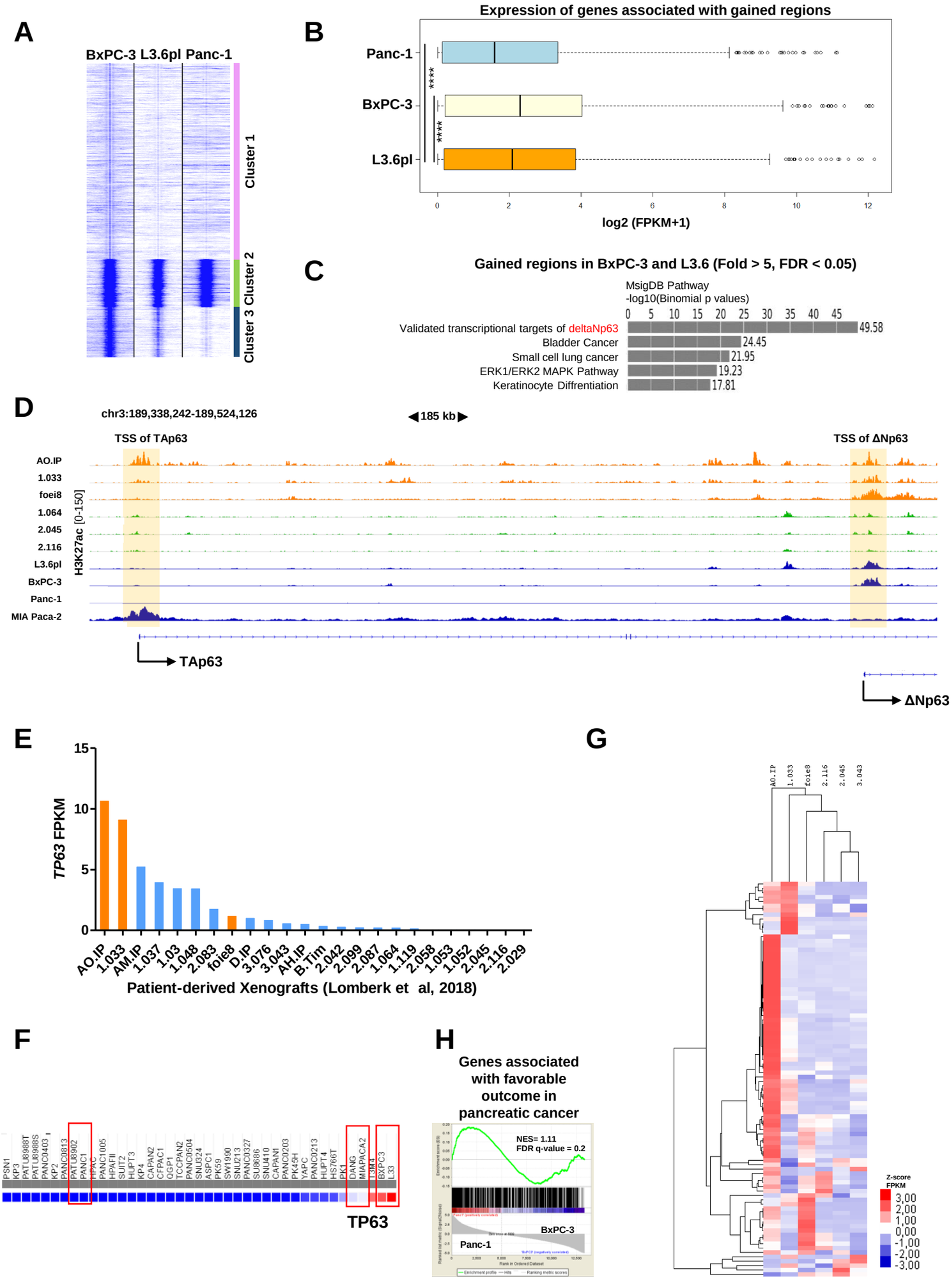

Supplementary Figure 2

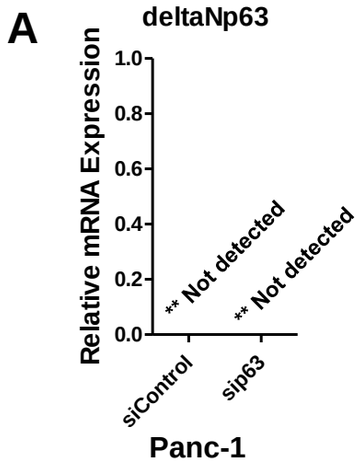

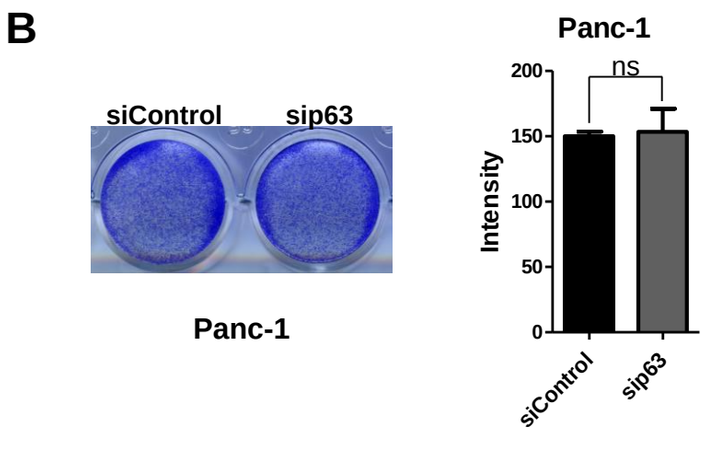

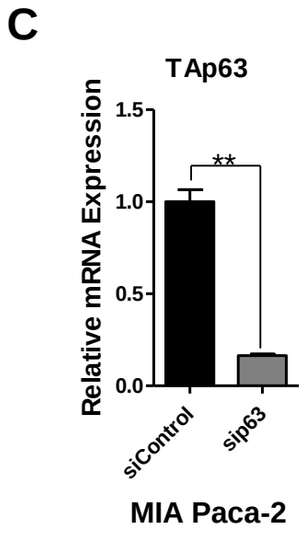

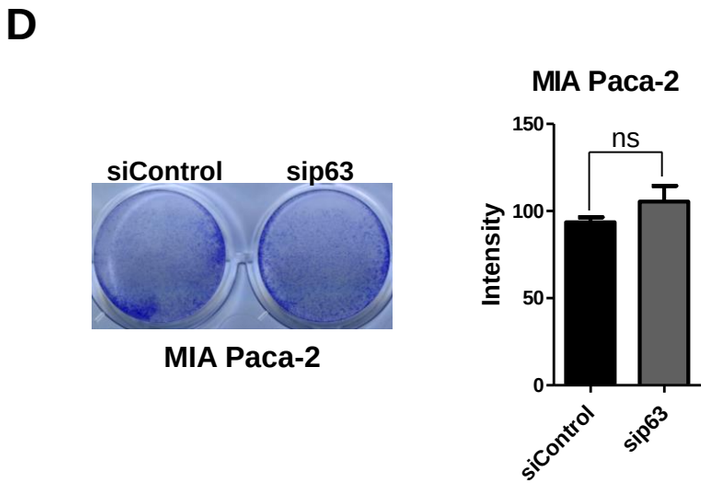

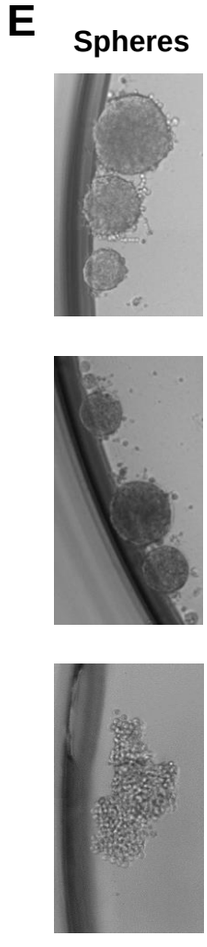

F GSEA Enrichment in siControl L3.6 cells compared to sip63

NAME	SIZE	ES	NES	FDR q-val
SCHUHMACHER_MYC_TARGETS_UP	78	-0.75943	-3.17847	0
MANALO_HYPOXIA_DN	283	-0.62011	-3.11342	0
WONG_EMBRYONIC_STEM_CELL_CORE	323	-0.57769	-2.91488	0
DANG_MYC_TARGETS_UP	132	-0.58907	-2.70979	0
HUPER_BREAST_BASAL_VS_LUMINAL_UP	46	-0.73074	-2.70709	0
RODRIGUES_THYROID_CARCINOMA_POORLY_DIFFERENTIATED_UP	606	-0.49343	-2.6682	0
FOURNIER_ACINAR_DEVELOPMENT_LATE_2	273	-0.53196	-2.66488	0
RAMALHO_STEMNESS_UP	197	-0.53356	-2.55144	0
RHEIN_ALL_GLUCOCORTICOID_THERAPY_DN	335	-0.48737	-2.4864	0
BILD_MYC_ONCOGENIC_SIGNATURE	195	-0.51516	-2.47975	0
BIDUS_METASTASIS_UP	204	-0.50879	-2.43919	0
YAO_TEMPORAL_RESPONSE_TO_PROGESTERONE_CLUSTER_11	93	-0.57496	-2.43622	0
RICKMAN_TUMOR_DIFFERENTIATED_WELL_VS_MODERATELY_DN	82	-0.57284	-2.37207	0
ELVIDGE_HYPOXIA_DN	135	-0.50709	-2.28979	0
KEGG_RIBOSOME	85	-0.55021	-2.28603	0
GROSS_HYPOXIA_VIA_HIF1A_UP	74	-0.55224	-2.2832	0
RICKMAN_TUMOR_DIFFERENTIATED_WELL_VS_POORLY_DN	335	-0.42365	-2.15112	6.24E-05

G GSEA Enrichement in sip63 L3.6 cells compared to siControl

NAME	SIZE	ES	NES	FDR q-val
LIN_SILENCED_BY_TUMOR_MICROENVIRONMENT	87	0.741889	3.093567	0
SENGUPTA_NASOPHARYNGEAL_CARCINOMA_DN	184	0.56477	2.63524	0
LIM_MAMMARY_STEM_CELL_DN	391	0.490658	2.472543	0
CHARAFE_BREAST_CANCER_LUMINAL_VS_MESENCHYMAL_UP	399	0.492597	2.471339	0
LIM_MAMMARY_LUMINAL_MATURE_UP	82	0.584894	2.398431	0
BOSCO_EPITHELIAL_DIFFERENTIATION_MODULE	46	0.657135	2.390054	0
SMID_BREAST_CANCER_RELAPSE_IN_BONE_UP	55	0.598831	2.281816	7.76E-05
CROMER_TUMORIGENESIS_DN	34	0.64979	2.244613	7.33E-05
ODONNELL_TARGETS_OF_MYC_AND_TFRC_UP	53	0.596211	2.233752	5.5E-05
SMID_BREAST_CANCER_LUMINAL_B_UP	103	0.523645	2.228037	5.28E-05
SMID_BREAST_CANCER_BASAL_DN	438	0.43851	2.226336	5.07E-05
VECCHI_GASTRIC_CANCER_ADVANCED_VS_EARLY_DN	93	0.527829	2.206488	7E-05
LIEN_BREAST_CARCINOMA_METAPLASTIC_VS_DUCTAL_DN	79	0.533576	2.177088	0.000105
CHARAFE_BREAST_CANCER_LUMINAL_VS_BASAL_UP	295	0.440284	2.153986	0.000178
DAUER_STAT3_TARGETS_DN	44	0.558594	2.014827	0.000859
MARTENS_TRETINOIN_RESPONSE_UP	271	0.412329	1.97972	0.001319
BIDUS_METASTASIS_DN	115	0.433148	1.864891	0.003689

Supplementary Figure 3

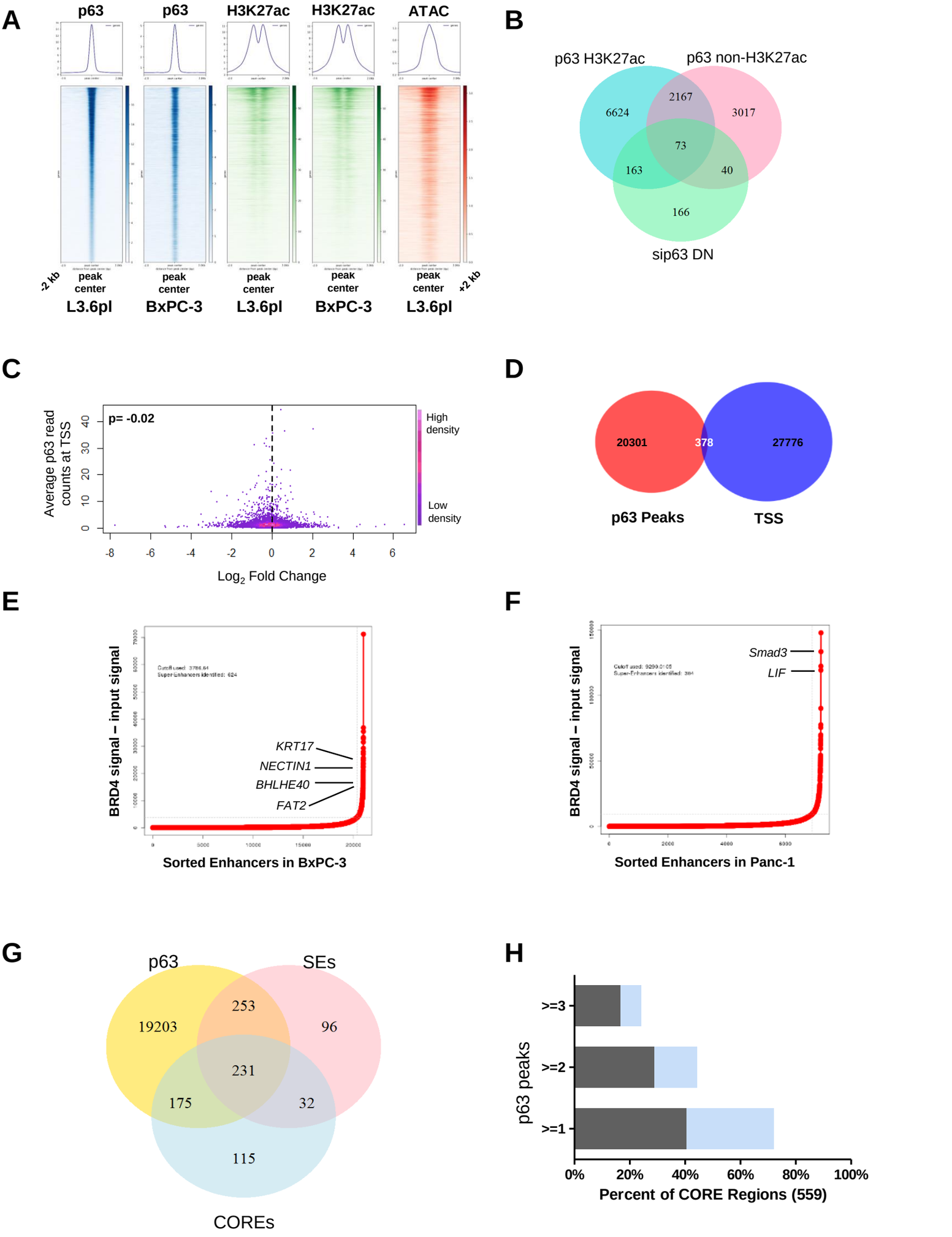

Supplementary Figure 4

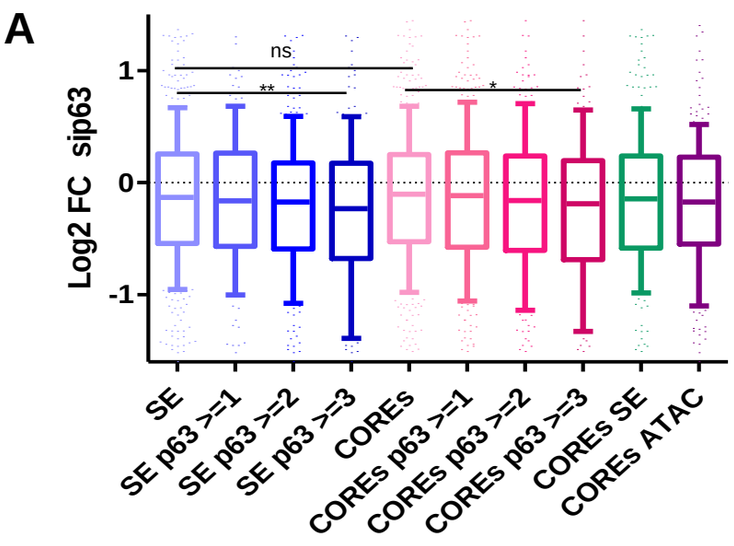

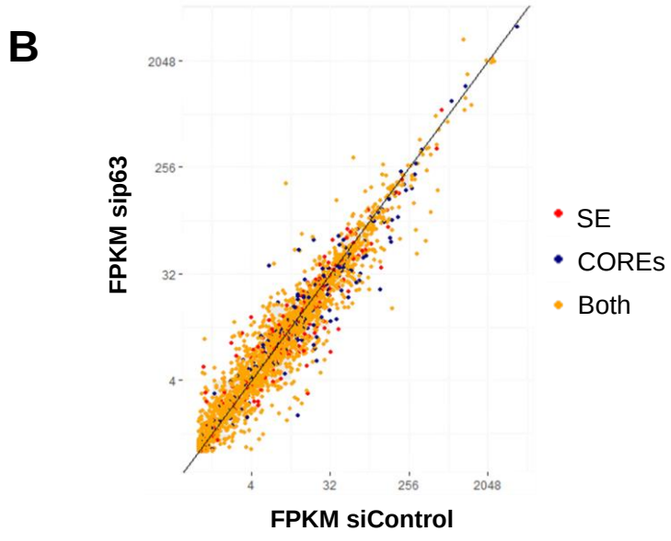

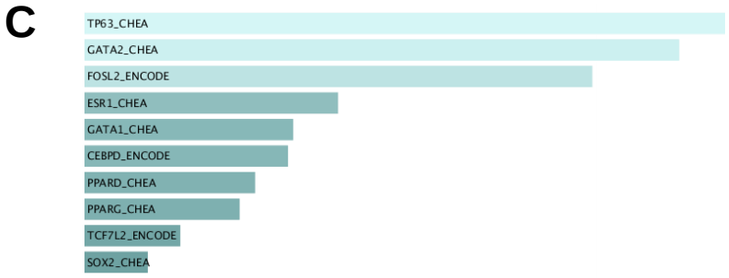

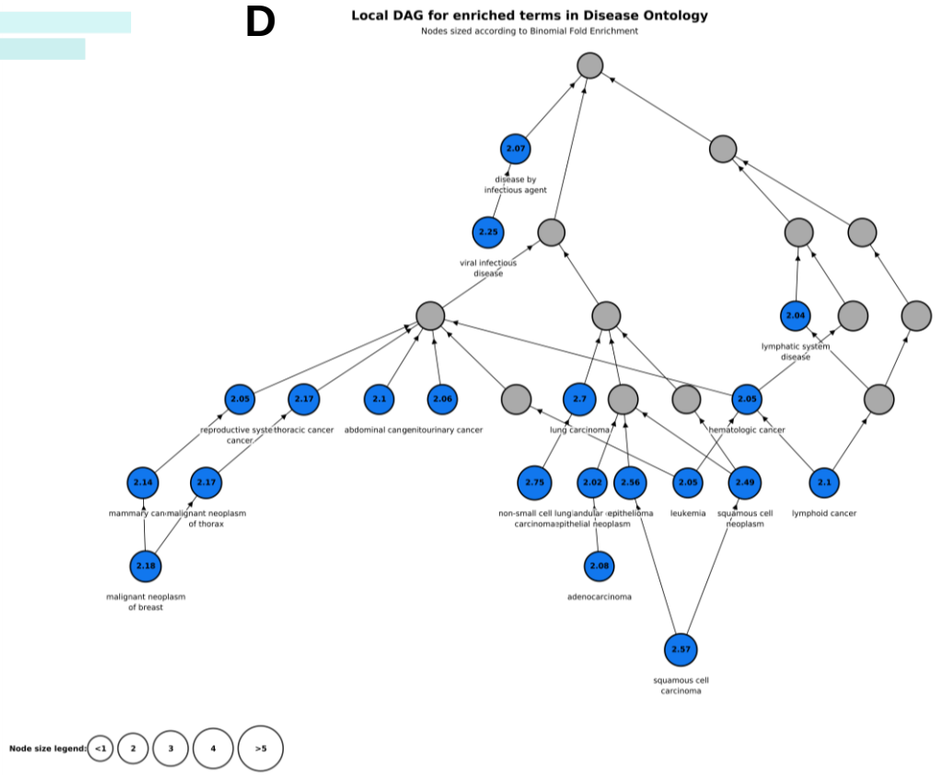

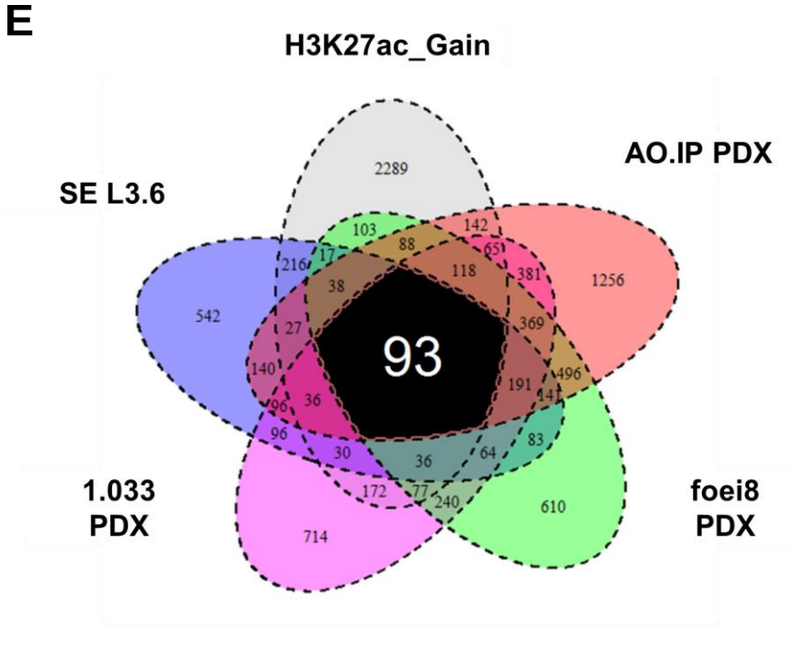

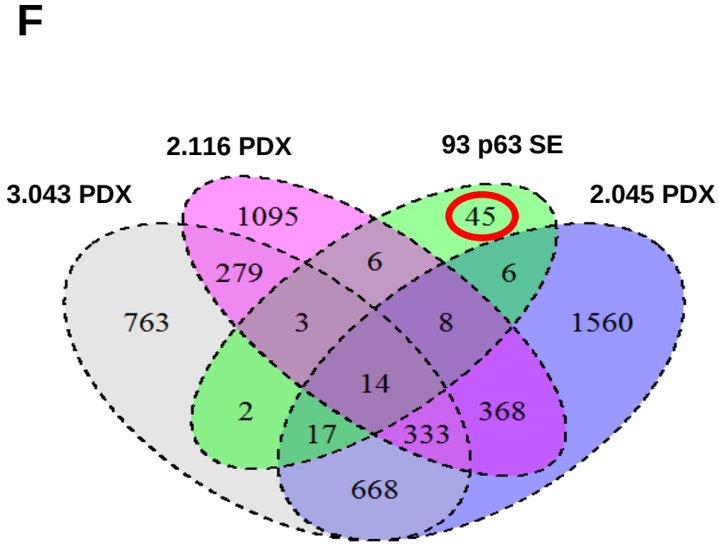

Supplementary Figure 5

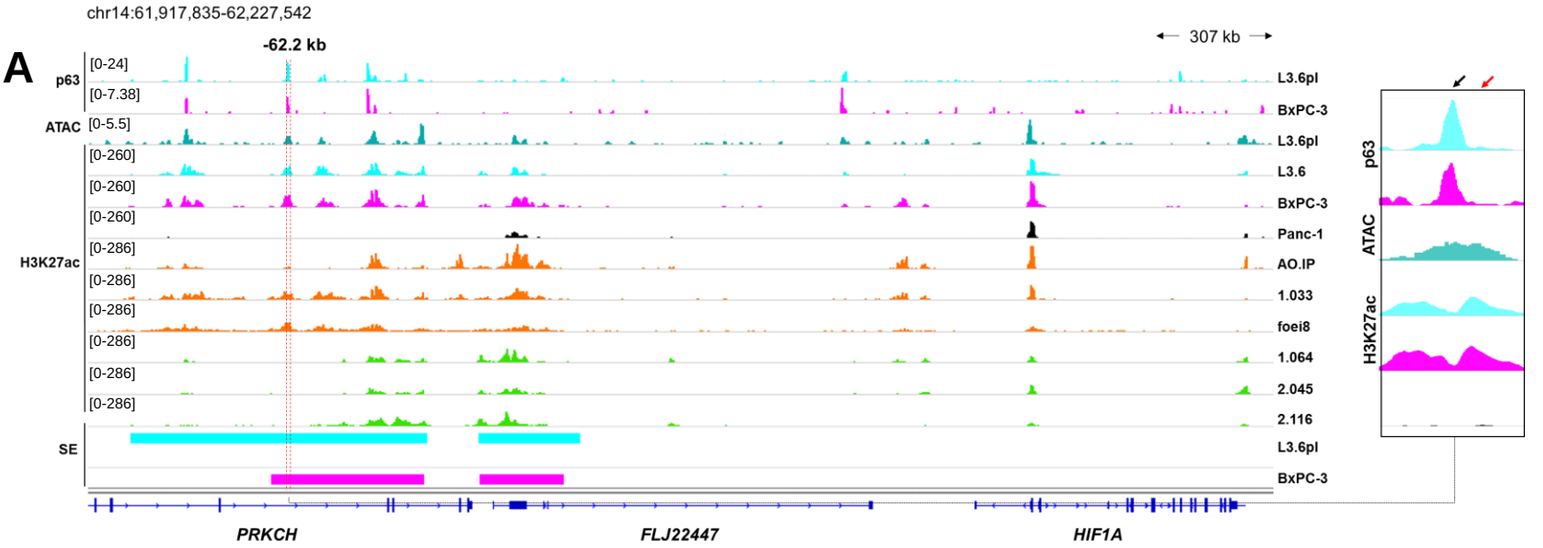

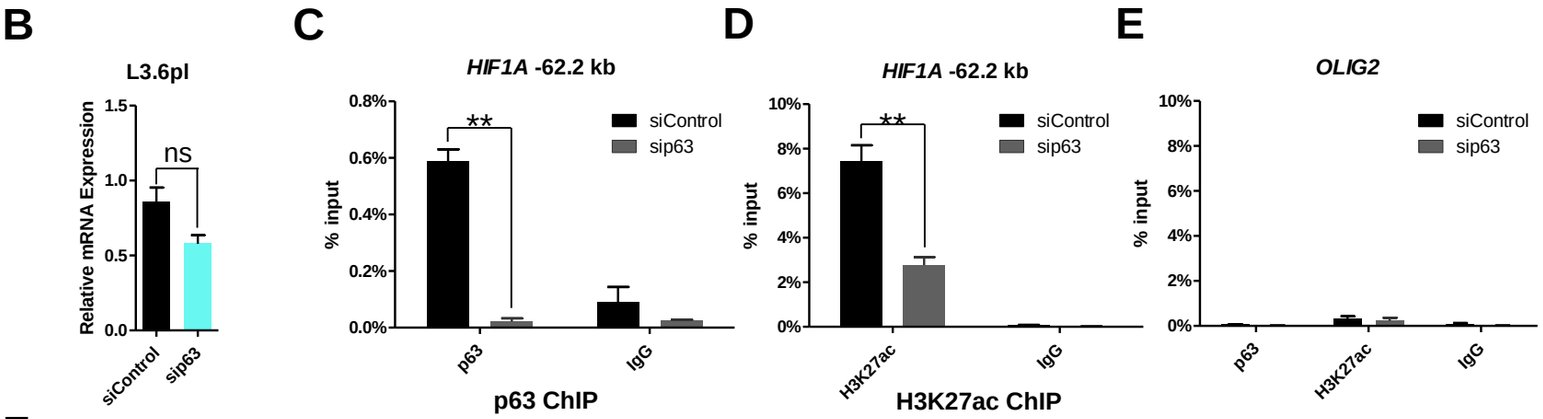

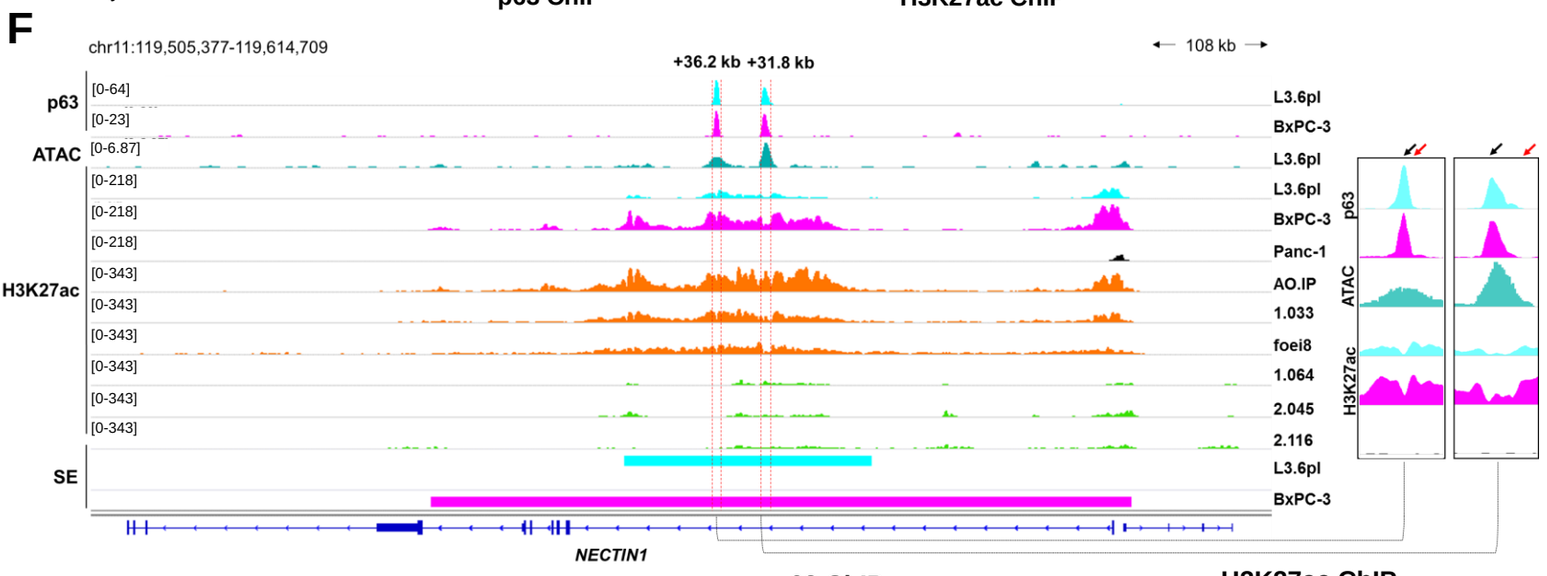

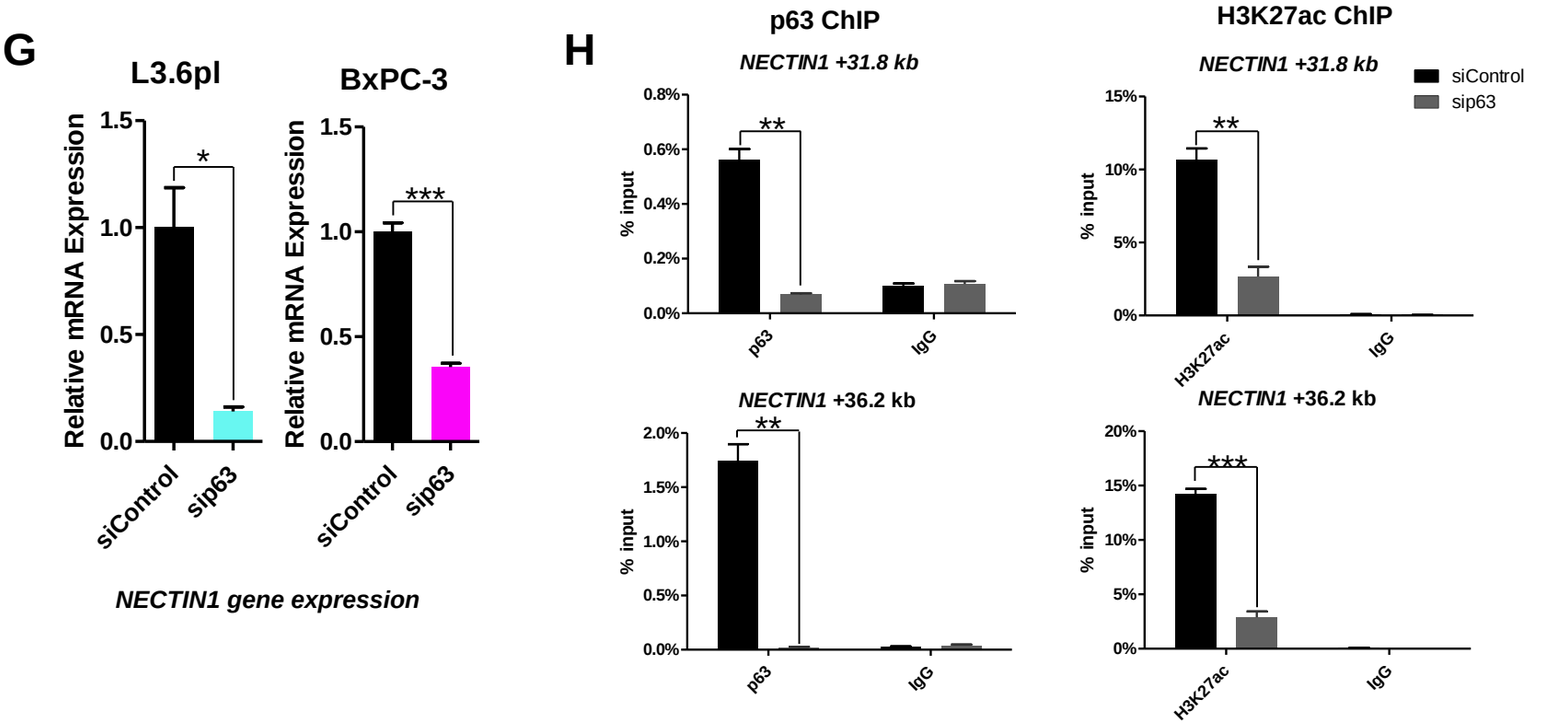

Supplementary Figure 6

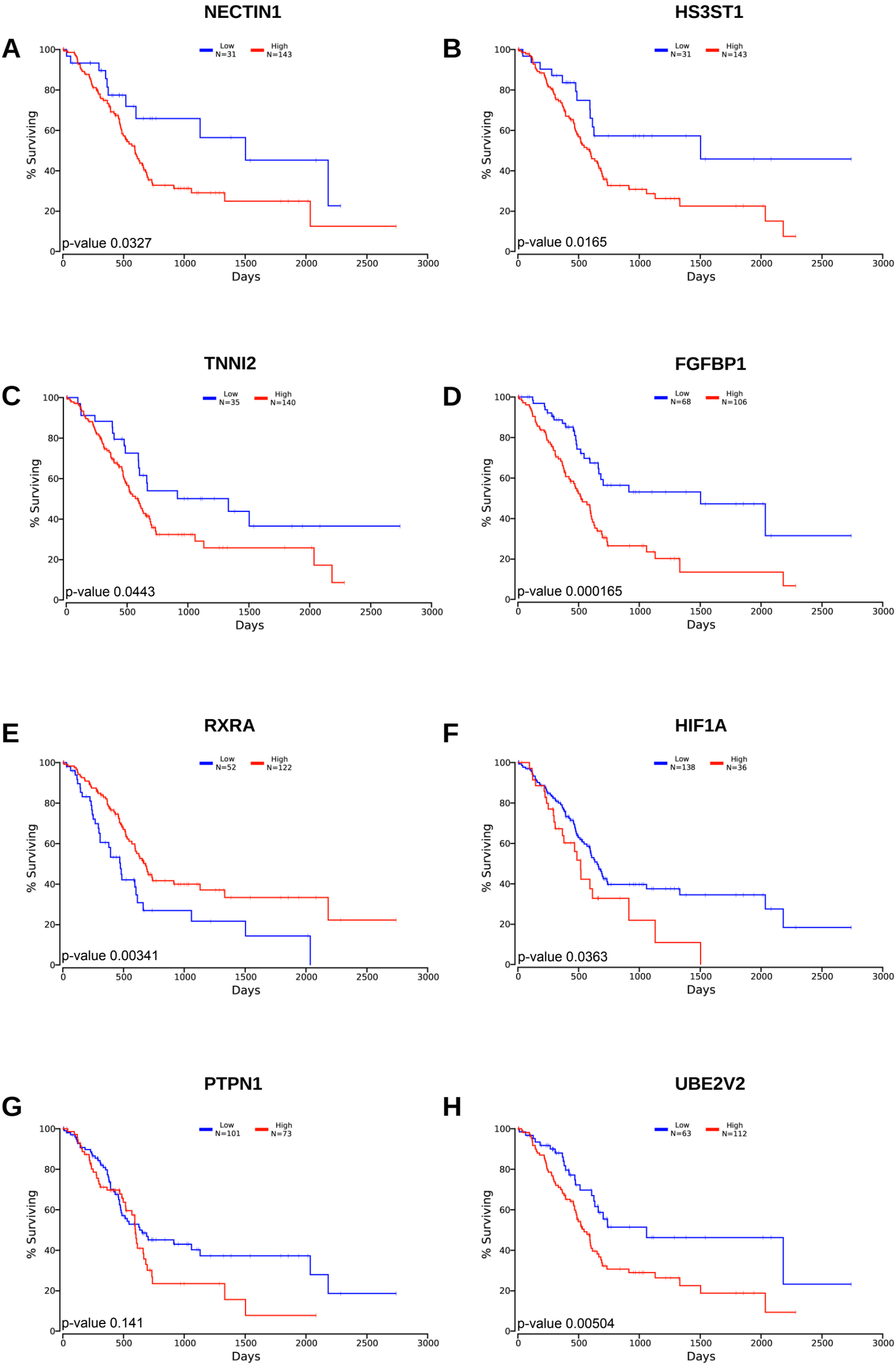

Supplementary Figure 7